HEAT RESISTANT LAMINATED COMPOSITES FROM METAL FOILS WITH PYRO-CARBON, SILICON-CARBON AND CARBIDE COATINGS

Valery P. Korzhov

Institute of Solid-State Physics of the Russian Academy of Sciences,
Chernogolovka, Moscow Region, Academician Osipyan Street, 2, 142432, Russia

Abstract

The work combines three different methods for producing coatings with carbon and silicon – pyrolytic carbon coating on niobium, solid-phase carbide coatings on metal foils using thermally expanded graphite, and silicon-carbon coating from the vapor phase. If the first and last coatings have been known for a relatively long time, the solid-phase method of applying carbide coatings to metal foils using TE-graphite tapes has been used only recently by us. A unifying factor is the solid-phase synthesis of heat-resistant layered composites using metal foils with coatings obtained by each of the methods described in this work as starting elements.

Keywords: *pyrocarbon, carbide coating, silicon coating, layered composite, solid phase method, diffusion welding, multilayer structure, intermetallic compound, solid solution, niobium carbide, strength*

1. INTRODUCTION

Alloys with predominantly directional structures are characterized by better strength properties compared to alloys having, for example, a cast structure. Therefore, directional crystallization technologies are constantly being improved [1–6]. When these methods are obtained by heat-resistant alloys, they strive to form such a sharply directed cellular structure in them [7], in which the cells consist of heat-resistant intermetallic phases, alternating with the structural elements of a solid solution based on an alloy-forming metal, responsible for the crack resistance of the material at room temperature.

A similar structure can be formed artificially if conditions are laid down for this at the initial stage of product formation. This applies to layered composites, which are the subject of the present work. It shows that metal foils with heat-resistant coatings are first prepared. And then packets are formed from foil with coatings intended for solid-phase production of heat-resistant layered composites.

In this work, the initial elements for the formation of multilayer packets were:

– Nb-foils with pyrolytic carbon coatings,

– foils of a Ti alloy, niobium, and an Nb–2% Zr alloy with carbide coatings prepared by solid-phase technology, and

– Nb-foil Si-coated vapor phase.

To obtain layered composites, packages were subjected to diffusion welding (DW) under pressure.

2. COMPOSITES OF Nb-FOILS WITH PYROCARBON COATING

2.1. Pyrocarbon coatings

We call pyrocarbon coatings thin films of pyrolytic carbon, which is formed on hot metal surfaces by the decomposition of hydrocarbons.

Since these coatings are obtained by pyrolysis in a very wide temperature range, their structures and properties cannot but depend on temperature. Therefore, in practice, there are low- and high-

temperature pyrocarbon coatings with temperature ranges of 750–1100 and 1400–2500°C, respectively [8].

Depending on the pyrolysis conditions, high- and low-density, highly anisotropic and practically isotropic pyrocarbon coatings are obtained, characterized by high thermal stability and lack of porosity. On the issue of the formation of pyrocarbon coatings, two concepts have long been competing. The first – the occurrence of pyrocarbon depends on volumetric processes. This is adhered to by J. Bokros [9, 10] and K. Makarov [11–14].

A second look at this – the formation of pyrocarbon does not depend on volume, but begins and continues exclusively on the surface. This approach is more combined with experiment and has more of its supporters. This is the work of P. Tesner and co-workers [15–22], according to which carbon is formed entirely on the surface and does not require preliminary stages in volume. In the presence of developed dispersed surfaces, the reaction proceeds towards the appearance of solid carbon and hydrogen. In a wide range of pressures and temperatures, according to Tesner's theory, the carbon formation reaction is of the first order in hydrocarbon pressure. The activation energy is kept constant and independent of temperatures. The growth of the pyrocarbon layer is determined by the simultaneous occurrence of two processes: the formation of crystallite nuclei and their growth. During growth, carbon atoms from the gas phase interact with the carbon of the nuclei, forming a dense mass. Growth goes through the so-called “growth cone”. The top of the cone “fits” into the substrate, and the direction of growth is oriented perpendicular to the surface of the substrate.

The bases of the cones gradually fill the entire surface of the substrate. Over time, the cones become cylinders and the columnar growth of the structure begins. Inside columnar crystallites, layers of carbon atoms are able to form, depending on the temperature at which growth occurs, either a turbostratic or graphite-like structure.

And a little about the widespread use of pyrocarbon:

– as a structural and crucible material in the production of semiconductors, glass, single crystals and pure metals,

– as anti-friction sealing and as erosion-resistant material,

– for volume sealing of brake pads made of carbon-carbon composites,

– as electrodes for chemical and spectral analysis,

– to obtain the material of the anodes of chemical current sources, including the anodes of lithium-ion batteries.

Pyrocarbon coatings are applied to the bow of the rocket and to the walls of the combustion chamber of rocket engines.

2.2. Pyrocarbon for heat-resistant layered composites of solid-phase manufacturing

The work uses a pyrocarbon coating on niobium foils in order to obtain layered heat-resistant Nb composites with carbide hardening. Pyrocarbon coatings were obtained on both surfaces of Nb-foils with a thickness of 50 μm as a result of decomposition of methane CH_4.

About 20 Nb foils ~35×45 *mm* in size could be fixed in the clip. At “the exit” received Nb-foil with a 2-sided pyrocarbon coating – CNbC. The ratio of the coating thickness to the niobium thickness t_C/t_{Nb} varied from 0,20–0,25 to 0,4–0,5 μm with a applied carbon coating thickness of 5–7 μm. The coating temperature was ~1100°C.

Two types of multilayer packets were formed from the obtained CNbC foils:

– Nb/CNbC or Nb/CNbC/Nb/CNbC/..., in which Nb foils with a 2-sided carbon coating were transferred by Nb foils without coating, and

– CNbC/CNbC or Nb/CNbC/CNbC /..., which were assembled from Nb foils with a 2-sided C-coating. In both packages, the outer were non-coated Nb foils.

For comparison, a multilayer Nb/Nb package was prepared, consisting of Nb-foils without pyrocarbon. The sintering temperature of the packets varied from 1150°C for the Nb/Nb packet to 1200 and 1300°C for the Nb/CNbC and CNbC/CNbC packets, respectively. A positive result at these temperatures was achieved with exposure for 1–2 hours and even 30 minutes. Pressure varied over a fairly wide range – from ~8 to ~30 *MPa*. The thickness of the bags after welding changed slightly.

2.3. Structures of composites of Nb foils with pyro-carbon coatings

The cross-sectional structure of the composite obtained by diffusion welding of the Nb/CNbC package, in which CNbC foils alternated with uncoated Nb foils, is shown in Fig. 1. It is seen that in the composite one "pyro-carbon layer" was located between two Nb layers. It is important to note that the Nb layers with pyro-carbon coatings looked bright, and the niobium layers without coatings had many gray inclusions inside, which were most likely niobium carbides.

At a larger increase (Fig. 2), according to the data of local X-ray spectral analysis, a 2-phase zone of a continuous and dense dark gray layer of Nb_2C carbide ~6 *μm* thick and an island layer of the NbC_{1-x} carbide phase of black colors was detected at the interface of two Nb-foils. The layer identified as Nb_2C carbide contained from 5,2 to 6,3 wt.%C and 93,7–94,8 wt.% Nb. The formation of black NbC_{1-x} carbide is from 12,2 to 13,1 wt.% C and 86,9–87,8 wt.% Nb. The layers designated as (Nb), as a result of carbon diffusion, became after welding a solid solution of carbon in niobium.

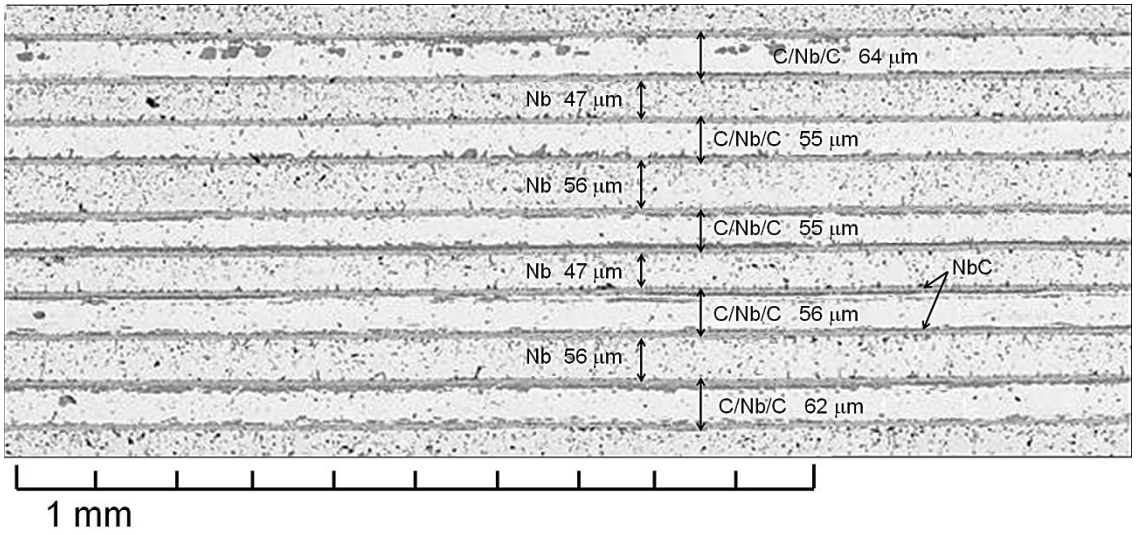
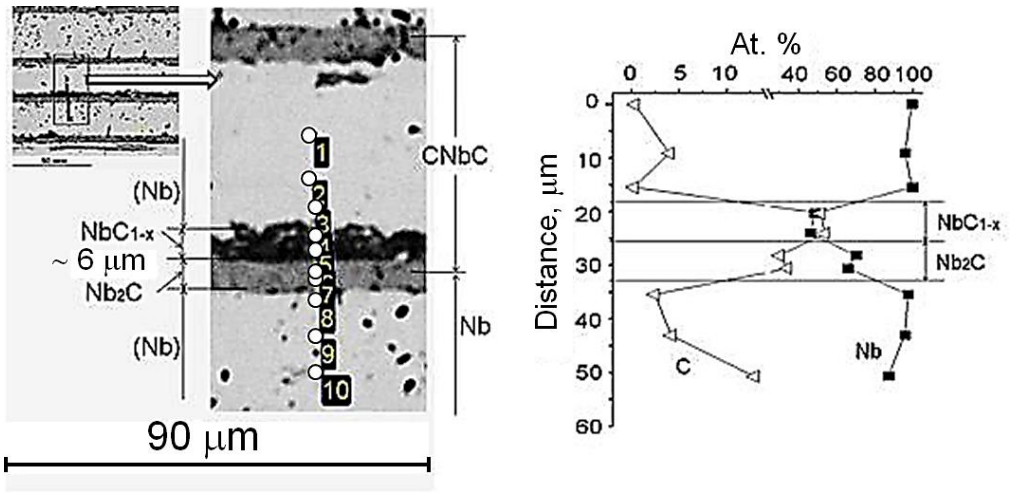


Fig. 1. The macrostructure of the cross section of the Nb/CNbC package along the rolling direction of the Nb-foils. Diffusion welding – at 1200°C for 1 *h*



a *b*

Fig. 2. Fragment of the microstructure of the Nb/CNbC composite after DW (*a*) and concentration profiles of Nb and C of the diffusion zone between two adjacent Nb-layers (*b*): (Nb) – solid solution of C in Nb, 1–10 – spectrum numbers

A significant consequence of the diffusion welding of Nb/CNbC packets was this result. Judging by the concentration profiles of Nb layers, on the both sides of the carbide phase (see Fig. 2*b*), the Nb layer, which had a 2-sided pyrocarbon coating, contained from 0 to ~ 7 at.% C after welding. And in the Nb-layer without coating, the carbon content was from 5 to 12,5 at.%. This means that in the process of diffusion welding, the diffusion of carbon occurred to a much greater extent in the Nb-foil without coating than in the foil that had pyrocarbon coatings!

A confirmation of the fact that carbon from the pyrocarbon layer does not diffuse into the niobium substrate was the bright contrast of Nb layers in the CNbC/CNbC composite, composed only of Nb foils with 2-sided pyrocarbon coatings (Fig. 3).

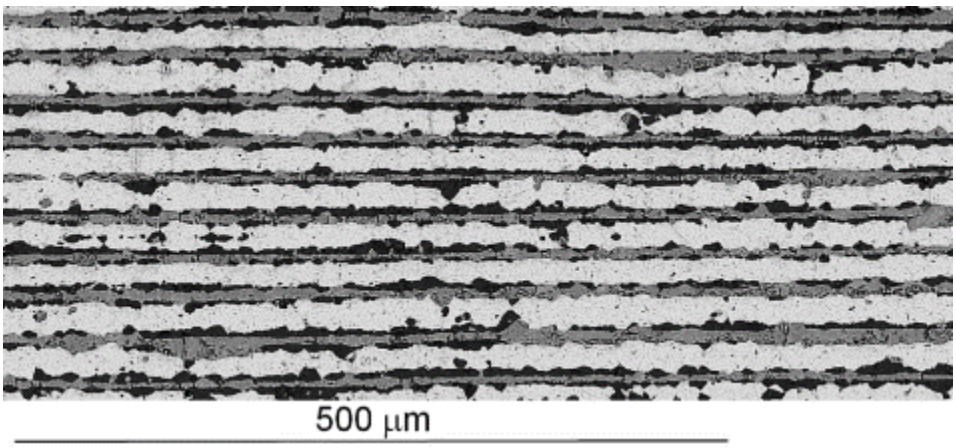
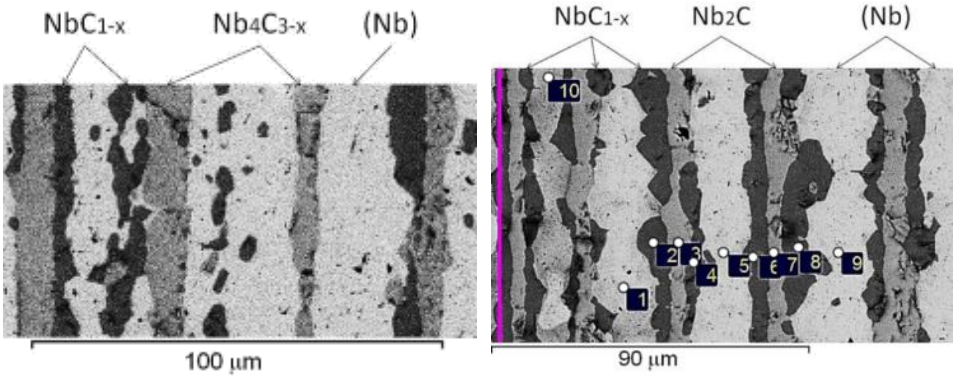


Fig. 3. The cross-sectional structure of CNbC/CNbC composites along the direction of rolling of Nb-foils after diffusion welding according to the mode: 1500°C, 2 *h*, ~33 *MPa*

Consider the microstructure of two CNb/CNbC composites obtained from identically assembled multilayer packets. In such composites, two layers of pyrocarbon fall into two Nb layers. Both packages were welded at 1500°C, but differed in welding time and pressure: 30 *min* and ~8 *MPa* in

comparison with 2 *h* and ~33 *MPa*. The cross sections of both packets had layered structures (Fig. 4), characterized by a strict alternation of light and gray layers, of which the gray layers were noticeably smaller in thickness. On the boundaries between the layers there were island inclusions of various shapes and lengths located on both its boundaries, and in the case of a composite with a 30-minute welding, also inside light layers. If we characterize the behavior of the black phase, then in a composite with 2-hour welding it is more, and it is more consolidated than in a composite with less rigid welding modes.



a *b*

Fig. 4. Microstructure of multilayer composites CNbC/CNbC 1 and 2 after welding at 1500°C for 30 *min* and under a pressure of ~8 *MPa* (*a*) and for 2 hours under a pressure of 33 *MPa* (*b*): 1–10 – analysis points

2.4. Discussion of the results of local X-ray spectral analysis

Table 1 shows the volumetric contents of structural components for composites of both configurations after diffusion welding, calculated from microphotographs in the mode of secondary electrons with material contrast. Immediately, we note that the amount of carbide component in the Nb/CNbC composite, equal to 12 %, is significantly less than in the CNbC/CNbC composites. This is understandable, since the ratio of the thicknesses t_C/t_{Nb} in it is 0,2–0,28 if compared with 0,4–0,5 for CNbC/CNbC composites. True, the welding temperature for the Nb/CNbC composite was 1200, and for the CNbC/CNbC composite – 1500°C. But we believe that for the volume fraction of hardening phases, the determining factor is still the ratio t_C/t_{Nb}.

Table 1. The volumetric content of the structural components of the composite, %

Structural component	Nb/CNbC: 1200°C, 1 *h*	1CNbC/CNbC: 1500°C, 30 *min*	2CNbC/CNbC: 500°C, 2 *h*
(Nb)	88,0	66,4	50,4
Nb_4C_{3-x}		24,7	
Nb_2C			30,1
NbC_{1-x}		8,9	19,6
Nb_4C_{3-x} + NbC_{1-x}		33,6	
Nb_2C + NbC_{1-x}	12,0		49,7

Let us compare the volume contents of carbide components in the 1CNbC/CNbC and 2CNbC/CNbC composites. They have the same ratios t_C/t_{Nb}, but differ in welding times and pressures. The total amount of carbides in the composite with 2-hour welding was 1,5 times greater than in the composite after welding for 30 minutes. But it happened mainly due to an increase in the volumetric content of NbC_{1-x} carbide – 2,2 times (19,6 / 8,9 = ~2,2). Moreover, the increase in the content of carbide components with a lower carbon concentration was only 1,2 times (30,1 / 24,7 = ~1,2).

The last observation follows from the experimental result, which is not consistent with the general concepts of reactive diffusion and, in particular, with our work on solid-phase composites with the participation of elements of the Nb–Al system. In [23–25], the development of the structure of the Nb/Al composite proceeded in the direction from an intermetallic compound with the highest aluminum content, such as $NbAl_3$ in the Nb–Al system, to a compound with a lower content of a low-melting component, Nb_3Al, and ended with a α-solid solution of aluminum in niobium The diffusion interaction zone between Nb and Al represented the following sequence of intermetallic phases: $NbAl_3$ → Nb_2Al → Nb_3Al → α, where α is a solid solution of Al in Nb. In the Ti/Al composite, the interaction zone had a similar orientation of intermetallic interchangeability: $TiAl_3$ → $TiAl_2$ or Ti_2Al_5 → TiAl → Ti_3Al → α-Ti. Due to the fact that the source of aluminum is limited to a much greater extent than niobium and titanium, the intermetallides of niobium and titanium with the highest Al concentrations were present only at the initial stage of diffusion welding. On the border with solid aluminum solutions in Nb or Ti, each time there were compounds with the lowest aluminum contents – Nb_3Al or Ti_3Al, respectively. It could be stated that the evolution of phase structures in these systems during the mutual diffusion of components occurs from intermetallic compounds with the highest Al content to its corresponding solid solutions in metals.

After welding, we observed two phase sequences in composites of niobium with carbon: Nb_2C → NbC_{1-x} → Nb) and Nb_4C_{3-x} → NbC_{1-x} → (Nb) (see Fig. 4, *a* and *b*). In the Nb/Al and Ti/Al composites, the aluminum concentrations in the intermetallic compounds in the direction from left to right decreased monotonically, and in the Nb/C composites, the changes in carbon concentrations were nonmonotonic. Between carbides with carbon concentrations of ~33 or ~43 at.% and Nb-solid solutions (Nb) with the lowest carbon content, NbC_{1-x} carbide with ~50 at.% C was "wedged".

Such a result can be explained by the formation of discrete formations of niobium monocarbide already at the stage of applying the pyrocarbon coating.

This is quite possible, since it is known that carbon atoms have high mobility, and even at temperatures above 650°C the diffusion coefficient of carbon becomes greater than the diffusion coefficient of metal atoms [26]. Thus, even short pyrocarbon coating times could be sufficient for the primary formation of NbC. The initial reason for this conclusion was the local presence of the NbC_{1-x} phase (see Fig. 2, *a*) in niobium, which had pyrocarbon coatings on both surfaces before diffusion welding, and its absence in uncoated niobium.

The final confirmation of this version was given by X-ray diffraction analysis of the Nb-surface with a pyrocarbon coating. It turned out that in addition to carbon and the Nb-solid solution, the spectrum contained lines of the cubic phase NbC: {111}, {200}, {220}. Moreover, an orthorhombic modification of the Nb_2C phase was also detected. The fact that continuous layers of Nb_2C or Nb_4C_{3-x} carbides were observed in the composite structure was already a continuation of the onset of interaction between the pyrocarbon coating and niobium. The observed increasing formation of the carbide phase NbC_{1-x} (see Table 1 and Fig. 2, *a*; 4, *a* and *b*) was the consolidation of its primary formations and the development of the interaction between it and Nb_2C (or Nb_4C_{3-x}).

2.5. Results of mechanical tests

Comparative strength tests for all Nb-foil composites with pyrocarbon coatings, as well as for comparing a multilayer composite of niobium foils Nb/Nb without coating, were carried out at room temperature (Table 2). As expected, the proportionality stress of the CNbC/CNbC composites containing a sufficiently large amount of the carbide component exceeded 900 *MPa* and significantly exceeded the σ_{PR} of the Nb/Nb and Nb/CNbC composites, but the fracture nature in the 1CNbC/CNbC

composite was fragile. The fracture of the 2CNbC/CNbC composite was characterized as pseudoplastic. This meant that, before the sample was destroyed, the experimental curve P(Δ), where P and Δ are the load and displacement, had a deviation from its linear dependence, extending much higher than the P_{PR}.

Table 2. Results of mechanical tests at room temperature

Composite	σ_{PR}, *MPa*	σ_B, *MPa*	Nature of destruction
Nb/Nb	290 ± 9	323 ± 49	Plastic
Nb/CNbC	253 ± 11	572 ± 38	Plastic
1CNbC/CNbC	–	979 ± 12	Fragile
2CNbC/CNbC	936 ± 94	1020 ± 94	Pseudoplastic

The results of short-term mechanical temperature tests for 3-point bending conducted for the 1CNbC/CNbC composite are shown in Fig. 5.

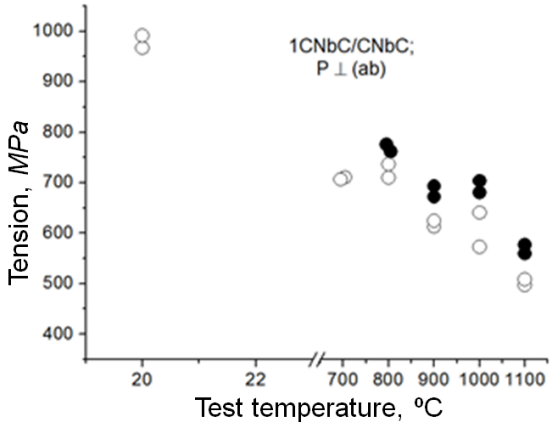


Fig. 5. Dependences of σ_{PR} (○) and σ_B (●) on the test temperature for 1CNbC/CNbC composite at P ⊥ (*ab*), where: P is the load and (*ab*) are the plane of the layers in the composite

The load P was applied perpendicular to the plane of the layers (ab) in the composite. The brittle nature of the destruction of the composite, observed at room temperature, was maintained at 700°C, but then it acquired a pseudoplastic character. On the load-displacement curves, it was possible to determine the proportionality stress σ_{PR}, which in the temperature range from 700 to 1100°C dropped from ~710 to 495–510 *MPa*, respectively. The strength σ_B at 1100ºC was 550 *MPa*.

Conclusions

- The preparation of a pyrocarbon coating on Nb-foils was developed, which was used as the main elements for the formation of multilayer packets for solid-phase preparation of composites with satisfactory strength values at room temperature (Nb/CNbC and 2CNbC/CNbC composites, see Table 2) and high fracture resistance characteristics at temperatures from 700 to 1100ºC (see Fig. 5). For Nb/CNbC and 2CNbC/CNbC composites, it was possible to determine the proportional stress, which indicated that they had a certain level of crack resistance.
- The structure of the composites was characterized by the alternation of layers of a solid solution of carbon in niobium and layers consisting of carbides NbC_{1-x} and Nb_2C or NbC_{1-x} and Nb_4C_{3-x}.

- NbC and Nb_2C carbides were already formed when a pyrocarbon coating was deposited on the surface of niobium. This assumption is based on the analysis of the microstructure of the cross section of the packets after diffusion welding and was confirmed by the data of X-ray diffraction analysis of the Nb surface with a pyrocarbon coating. As a result of welding, the formation of continuous layers of Nb_2C (or Nb_4C_{3-x}) was a continuation of the fast-flowing interaction of carbon with niobium, and the increasing amount of NbC_{1-x} monocarbide was a product of the consolidation of its primary formations and the beginning of the diffusion reaction between it and Nb_2C (or Nb_4C_{3-x}).
- The proportionality stress at room temperature of such composites was 935–980 *MPa*, and the σ_{PR} of a multilayer Nb/Nb composite, hardened only by "weak boundaries" between layers, made for comparison, did not exceed 290–300 *MPa*. At 1100°C, a composite with a multilayer structure containing 33,6 vol% of carbide layers had σ_{PR} = 495–510 *MPa*. Due to the preliminary nature of the research, this result is highly appreciated.

3. SOLID-PHASE METHOD FOR PRODUCING DOUBLE-SIDED CARBIDE COATINGS ON METAL TAPES

3.1. Brief characteristic of the method

In fact, such coatings belong to the category of diffusion coatings, which differ in the way the coating material is applied to the metal surface. Of the known methods, this is saturation of a metal surface with a coating material from

– powder mixtures,

– gas media (direct-flow and circulating methods),

– molten metals or their salts containing a diffusing element,

– pastes and suspensions (slip method).

In the proposed method, the saturation of the metal surface with carbon is a tape of thermally expanded graphite (TEG), but in the literature – exfoliated graphite. The method is characterized by simplicity, affordability and effectiveness.

In the solid-state method, using thermally expanded graphite (TEG) ribbons, it is easy to obtain carbide coatings on foils of any metals capable of forming carbide compounds with carbon. Despite the temperature limitations, and TEG is standardly applicable only at temperatures from -200 to + 400°C, in cases where the material is "closed" in the structure with a seal against oxidation, it can be used at temperatures up to 2000–2500°C. In this regard, here we use TE-graphite tapes as spacers between metal Nb-tapes, that is, in a "closed" design, to obtain carbide layers on them.

The sequence of basic operations for obtaining segments of metal tapes with a 2-sided carbide coating is as follows: (1) assembly of a package of 10–20 tapes, for example, from niobium, several tens of microns thick, and TEG tapes, (2) heat treatment (HT) under pressure P up to 15 *MPa* at 1500°C for 15–60 *min* (Fig. 6) and (3) disassembly of the package along the boundaries between two layers of TE-graphite.

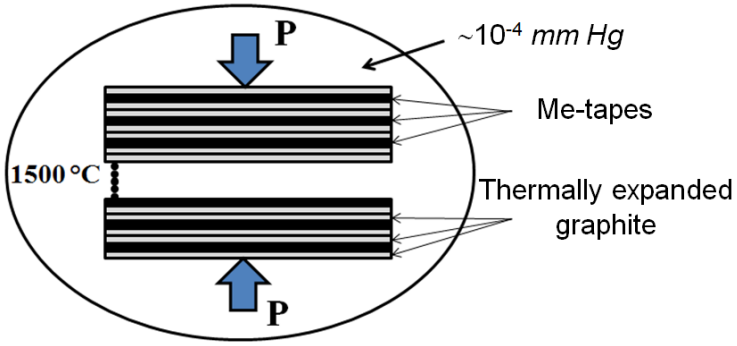
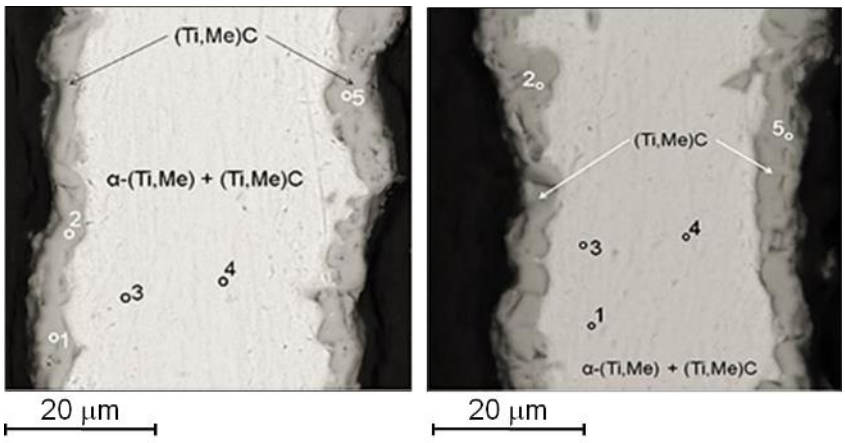


Fig. 6. Schematic illustration of the package and diffusion production of NbC coatings on Nb tapes

3.2. Carbide coatings on Ti-alloy tapes

The composition of the tape made of Ti alloy: Ti–10,0% Cr–7,3% Mo–2,6 wt.% Al. The thickness of the resulting tapes at the μ*m*-scale was uneven, but the coating itself with a thickness of ~3,5 to 6–7 *μm* appears dense (Fig. 7). According to local X-ray spectral analysis, the coatings consisted of titanium monocarbide: (Ti,Me)C ≡ $(Ti_{1,18}Me_{0,01})_{1,19}C_{0,81}$ (Me – Cr, Al, Mo). According to the Ti–C diagram, the composition of the 72,5Ti–21,5Me–6,0 at.% C ribbons corresponded to its eutectic region α-(Ti,Me) + (Ti,Me)C, where α-(Ti,Me) – solid solution of carbon in a titanium metal matrix. The carbon concentration is close to the eutectic composition.



a *b*

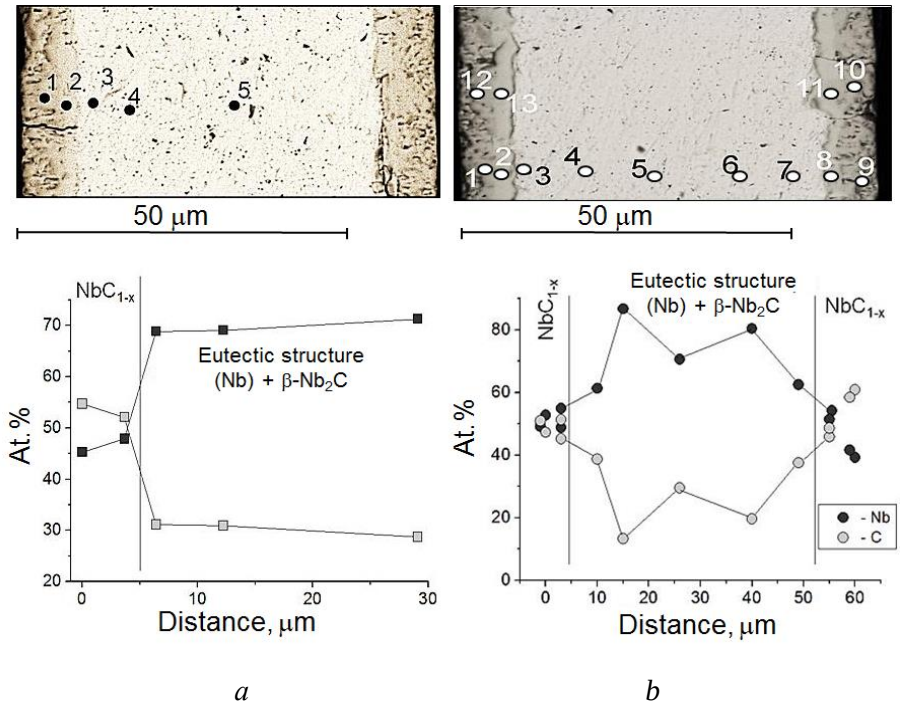
Fig. 7. The microstructure of the cross-section of the segments of the tape made of Ti-alloy after heat treatment (HT) under pressure at 1500°C for 15 *min*: 1–5 are points of analysis, and *a* and *b* – samples of tape bands after HT at pressures of 8 and 15 *MPa*, respectively

3.3. Carbide coatings on Nb tapes (Fig. 8)

The coatings consist of NbC monocarbide with compositions $Nb_{0,93}C_{1,07}$ and $Nb_{0,98}C_{1,02}$ on a tape 60 and 70 *μm* thick, respectively. During heat treatment of multilayer TEG/TEG/Nb/TEG/TEG/Nb packages, the volume of Nb ribbons was saturated with carbon to the composition of the eutectic region of the (Nb) + β-Nb_2C diagram, and NbC_{1-x} monocarbide coatings were formed on both surfaces of each ribbon.

After the heat treatment under pressure at a package 1500ºC for 1 hour on ribbons of coating were formed monocarbide NbC_{1-x}. According to the data of local X-ray spectral analysis, coatings on ribbons 60 and 70 *μm* thick had a slightly different composition - $Nb_{0,93}C_{1,07}$ and $Nb_{0,98}C_{1,02}$,

respectively. Unlike coatings on titanium foils (see Fig. 7), monocarbide coatings on niobium had the same thickness along the length of the foil. Unlike coatings on titanium foils (see Fig. 7), monocarbide coatings on niobium had the same thickness along the length of the foil – the NbC_{1-x} layer adjacent to the eutectic region (Nb) + β-Nb_2C, having a dense non-porous structure, and the outer layer with grains growing perpendicular to the surface of the substrate tape.



a *b*

Fig. 8. The microstructure and concentration profiles of the cross section of Nb-ribbons with a thickness 60 (*a*) and 70 *μm* (*b*) after solid-phase interaction with TEG tapes at 1500°C for 1 *h* and packet disassembly: 1–5 (*a*) and 1–12 (*b*) – number of spectra

Discrete precipitates of β-Nb_2C secondary carbide (Fig. 9) were visually observed in a 60 *μm* thick Nb tape (Fig. 9), most likely, as in a thinner substrate with a smaller volume. Although individual -Nb_2C carbide precipitates were also observed in ribbons 70 *μm* thick, which can be judged by the 5th point of the local X-ray spectral analysis (see Fig. 8,*b*), which led to a non-monotonic concentration dependence.

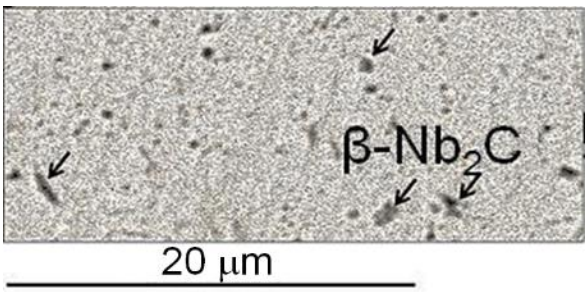


Fig. 9. The microstructure of the eutectic region of the Nb-tape with a thickness of 60 *μm* after heat treatment at 1500°C for 1 *h*

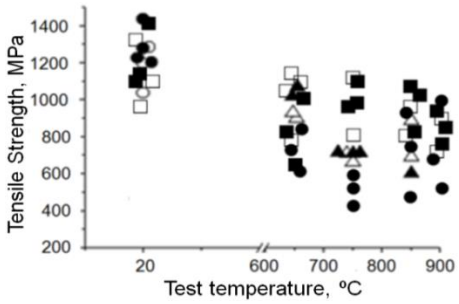
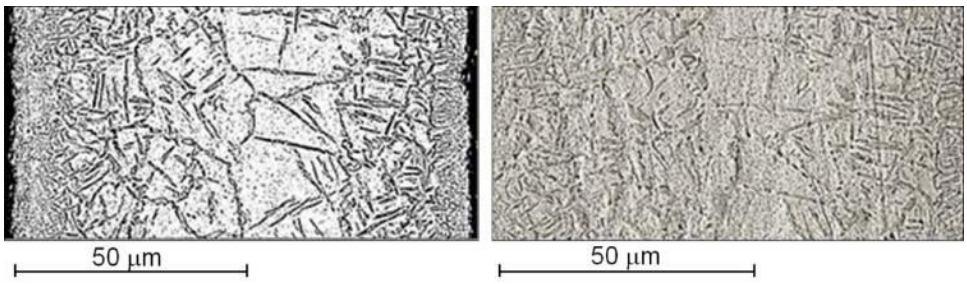


Fig. 10. Values of ultimate strength σ_{ST} of multilayer composites from metal tapes Ti-alloy (●, △, ▲) and niobium (■, □, ○) with carbide coatings after diffusion welding at 1250ºC, 2 *h*, 10 *MPa*

Ti/CTiC/CTiC ... and Nb/CNbC/CNbC ... multilayer packages were composed of titanium alloy tapes and niobium tapes with carbide coatings to obtain layered composites with only carbide hardening. Selected diffusion welding mode: 1250ºC for 2 hours at ~10 *MPa*. A fairly large set of strength tests was conducted for 3-point bending at 20°C and temperatures up to 900°C (Fig. 10). At room temperature, σ_B = 1000–1400 *MPa*, in the temperature range 650–900ºC – from 600 to 1100 *MPa*. These data are well combined with the strength for the 1CNbC/CNbC composite of pyrocarbon coated tapes (see Fig. 5).

3.4. Coatings on tapes made of Nb–2% Zr alloy (Fig. 11).



а *б*

Fig. 11. The microstructure of the cross section of the tape (Nb–Zr) alloy after heat treatment under pressure at 1500°C for 45 *min* in the secondary (*a*) and reflected electrons (*b*)

The material formed after heat treatment at 1500°C under pressure differed from all previous metal foils with coatings in that it did not have a carbide boundary layer similar to those observed on titanium alloy and niobium foils. The interaction of the (Nb–Zr) alloy foils with TE-graphite ribbons occurred without the formation of a continuous surface carbide layer as such. Near the surface and at a depth of 5–7 *μm*, finely dispersed Zr-based carbide precipitates were observed in the (Nb)-matrix: (Zr,Nb)C = $(Zr_{0,91}Nb_{0,20})_{1,11}C_{0,89}$. As they moved toward the middle of the tape, Zr carbide precipitates increased in linear size, extending into needles. The matrix phase was niobium-based carbide: $(Nb_{0,97}Zr_{0,15})_{1,12}C_{0,88}$ = $(Nb,Zr)C_{1-x}$.

Thus, we have a composite of 2 not crack resistant, but strong structural components – a matrix of carbide based on Nb and precipitates of carbide based on Zr.

The result was unexpected. However, it turned out that the foils themselves remained consolidated, “very brittle” did not collapse and withstand a bend of радиус10 *mm* radius!

It will be recalled to the place that the emerging problem of crack resistance, due to the presence of brittle compounds in the structure of the material, has long been considered insurmountable. For the first time, one of the possibilities for solving it was shown back in 1964 in [27] by braking cracks at a

weak interface between brittle phases. This idea was subsequently used in the development of various layered and fibrous composites [28, 29]. Therefore, it can be expected that the optimal organization of their structure with the alternation of brittle and relatively non-brittle carbide layers with relatively plastic layers of solid solutions of carbon and, possibly, silicon in niobium will be able to provide an acceptable level of crack resistance for the composite.

Conclusions

- For the first time by means of heat treatment under pressure of multilayer packets of thin foils of Ti alloy alternating with ribbons of thermally expanded graphite, continuous dense carbide coatings (Ti,Me)C (Me – Cr, Al and Mo) were obtained on the surfaces of metal foils. Similarly, coatings of NbC_{1-x} monocarbide were obtained on the surfaces of niobium foils.
- Diffusion welding under pressure of multilayer bags formed from carbide-coated foils produced laminated composites with structures of metal layers alternating with carbide layers that inherited carbide coatings. Tests of composites for bending strength showed that σ_B at room temperature reaches 1400 *MPa* and in the temperature range 650–900°C has values from 600 to 1100 *MPa*.
- The results on niobium foils with 2% zirconium are interesting in that, after diffusion welding of a package composed of such foils, the composite can be of scientific interest as an object in which crack braking will occur at a weak interface between brittle phases. According to theoretical data, such an effect is able to provide an acceptable level of crack resistance for the material. This should be facilitated by a carbide Nb matrix containing needle-like carbide inclusions based on zirconium.
- The coating method used can be modified to produce metal carbides functionally designed to be coated.

4. SILICON-COATED Nb FOIL COMPOSITE

4.1. Microstructure of the composite

The formation of silicon coatings on both surfaces of segments of Nb tapes with a thickness of 0,35 *mm* was carried out in Si vapor in a vacuum chamber with a graphite heater. Thanks to the heater, carbon from the CO atmosphere in the reactor chamber got into the coating. The temperature in the area of the foil was ~1500ºC. The time of the deposition process is 2,5 hours.

From the obtained niobium foils with (Si–C) coatings, packets for solid-phase production of a layered Nb/Si composite were made. Diffusion welding of packages was carried out at 1400°C for 1 *h* under a pressure of 9,5 *MPa*. The thickness of the composite of 5 foils after welding was 1,8 *mm*. The structure of its cross section is shown in Fig. 12.

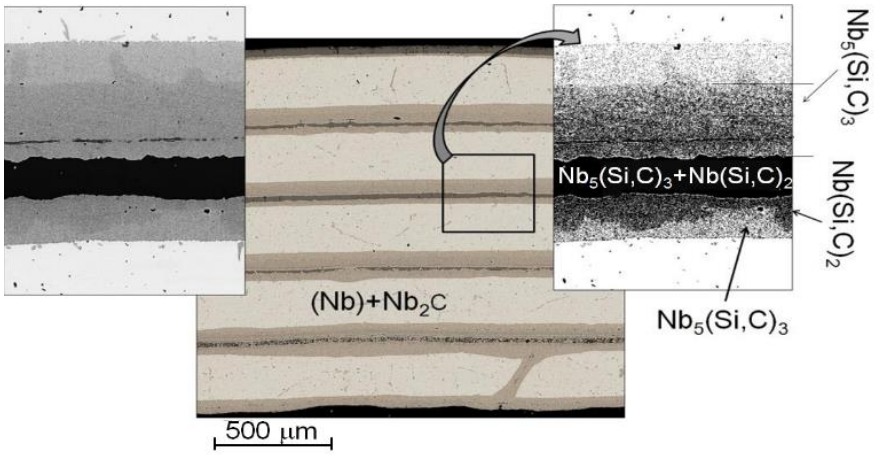


Fig. 12. Cross-sectional structure of a 5-layer Nb/(Si–C) composite after diffusion welding. Left and right – the interaction zone between two adjacent metal substrates in a normal light image (left) and with enhanced contrast (right)

The insets on the left and right reproduce the diffusion zone of interaction between adjacent layers. On the left – as it looks in ordinary light, on the right – processed by contrast methods using computer technology. The light layers inherited after diffusion welding of the Nb-foil contained ~10 at. % C. This corresponded to the 2-phase hypoeutectic region (Nb) + Nb_2C of the Nb–C diagram. It is important to note that these layers did not contain silicon at all (Fig. 13).

The interaction zone between two foils with Si coatings represented a diffusion region ~100 *μm* thick. According to the data of local X-ray spectral analysis in this zone, a dark layer with a thickness of ≤ 20 *μm* with a silicon content of 30 to 35 at.%, designated Nb_5Si_3 + $NbSi_2$, was reliably identified. Taking into account the concentrations of niobium and carbon (from 7 to 25 at.%), It can be concluded that the layer structure corresponds to the eutectoid region $Nb_5(Si,C)_3$ + $Nb(Si,C)_2$ of the hypothetical Nb–Si–C state diagram. The diffuse regions formed on both sides of the black layer (see Fig. 13) were asymmetric, which is clearly seen by their phase identification and light contrast (see Fig. 12).

The estimation of the volume contents of the viscous-plastic, and these are Nb-layers, and hardening phases gave such results – 63 and 37% for the matrix and intermetallic-carbide phases, respectively. The low content of hardening phases was reflected in the strength, which turned out to be relatively low (Fig. 14) in comparison with the composites Ti/CTiC/CTiC... and Nb/CNbC/CNbC...

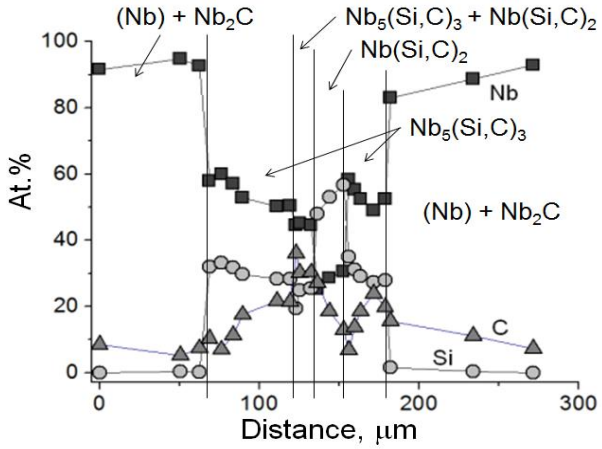


Fig. 13. Concentration profiles of Nb, Si and C of the interaction zone between two neighboring metal substrates

Fig. 15 shows the microstructure at the site of deformation of the composite, after testing for strength at 3-point bending. It is clearly seen that the cracks formed in the intermetallic-carbide interlayers during the tests effectively "quenched" in the crack-resistant layers with a eutectic structure.

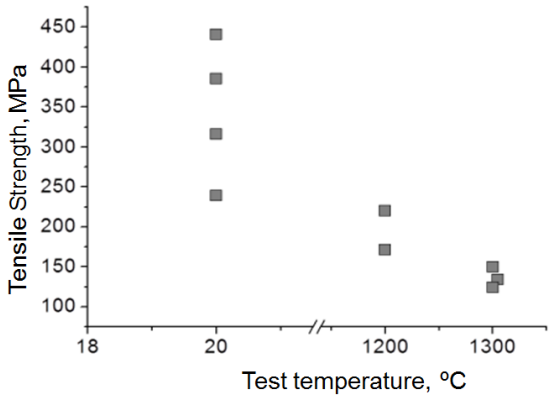


Fig. 14. The tensile strength of the composite at 20, 1200 and 1300ºC

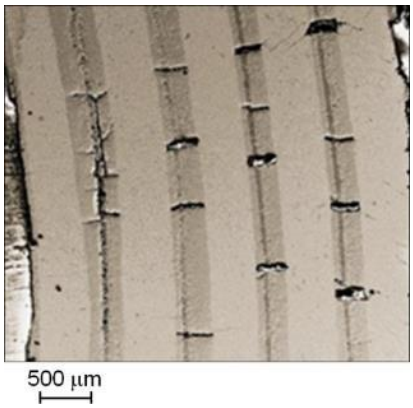


Fig. 15. The structure of the composite in the deformation zone corresponding to the point of application 3-point bending strength tests

Conclusions

- It has been shown that by vapor deposition in a reactor with a graphite heater, it is possible to obtain high-quality Si coatings with the addition of carbon on substrates of refractory metals, in particular, niobium. A test experiment was conducted on diffusion welding of a package of Nb-foils with Si-coatings and the layered structure of the obtained composite was studied. It was tested for bending strength at room temperature, 1200 and 1300ºC.
- A significant result of the research is the low penetration of carbon into Nb-foils. It can be hoped that this will make it possible for Si-coated metal foils to maintain high crack resistance even after the solid-phase process of obtaining layered composites from them.
- Moreover, in the light of recent trends in heat-resistant topics related to the interest in Mo alloys hardened by compounds with silicon and boron, there is an intention to use molybdenum instead of niobium in layered composites.

ACKNOWLEDGMENTS

At various times, young researchers A. E. Yershov, I. S. Zheltyakova, D. V. Prokhorov, and T. S. Stroganova took part in the presented work. I want to express my sincere appreciation to my young colleagues for all the years spent together - thank you very much for your respect, responsiveness and good relations.

REFERENCES

1. Jackson, MR, Bewley, BP, Rowe, RG, Skelly, DW, Lipsitt, HA 1996, "High temperature refractory metal-intermetallic composites", *J. Metals*, v. 48, no 1. pp. 39–44.
2. Bewley, BP, Jackson, MR, Subramanian, PR 1999, "Processing high temperature refractory metal-silicide in situ composites", *J. Metals*, v. 51, no 4, pp. 32–36.
3. Bewley, BP, Jackson, MR, Zhao, JC, Subramanian, PR 2003, "A review of very-high-temperature Nb-silicide-based composites", *Metall. Mater. Trans.*, v. A34, no 10, pp. 2043–2052.
4. Светлов, ИЛ, Абузин, ЮА, Бабич, БН, Власенко, СЯ, Ефимочкин, ИЮ, Тимофеева, ОБ 2007, "Высокотемпературные ниобиевые композиты, упрочненные силицидами ниобия", *Журнал функциональных материалов*, т. 1, №2, сс. 48–53.
5. Колобов, ЮР, Каблов, ЕН, Козлов, ЭВ, Конева, НА, Поварова, КБ, Грабовецкая, ГП, Бунтушкин, ВП, Базылева, ОА, Мубояджян, СА, Будиновский, СА 2008, *Структура и свойства интерметаллидных материалов с нанофазным упрочнением*. М.: ИД МИСиС, –328 с.
6. Коржов, ВП, Карпов, МИ 2009, "Структура жаропрочных сплавов системы Nb–Si с 3 и 6% (мас.) Si, полученных зонной плавкой", *Материаловедение*, №11, сс. 39–43.
7. Карпов, МИ, Внуков, ВИ, Коржов, ВП, Строганова, ТС, Желтякова, ИС, Прохоров, ДВ, Гнесин, ИБ, Кийко, ВМ, Колобов, ЮР, Голосов, ЕВ, Некрасов, АН 2012, "Структура и механические свойства жаропрочного сплава системы Nb–Si эвтектического состава, полученного методами направленной кристаллизации", *Деформация и разрушение материалов*, №12, сс. 2–8.
8. Кузнецов, ВГ, Пониматкин, ВП, Прокофьев, АВ 2010, "Нанесение пироуглеродных покрытий разложением углеводородов под действием плазмы вакуумно-дугового разряда", Вакуумная *техника и технология*, т. 20, №4, сс. 12–16.
9. Bokros, JC 1969, "Deposition, structure, and properties of pyrolytic carbon". In: Walker PL., editor. *Chemistry and physics of carbon*, v. 5. New York: Dekker; pp. 1–118.
10. Bokros, JC 1965, "The structure of pyrolytic carbon deposited in a fluidized bed Carbon", v. 3, Iss. 1, pp. 17–20.
11. Макаров, КИ, Полякова, КИ, Соловьев, ЕА 1963, "Кинетика термического разложения метана", *Газовая промышленность*, № 8, сс. 40–48.
12. Makarov, KI, Pechic, VK 1969, "Kinetics of methane thermal decomposition on the carbon surface in transient regime", *Carbon*, v. 7, no 2, pp. 279–285.
13. Makarov, KI, Pechic, VK 1974, "Kinetics of methane pyrolysis under conditions of pyrolytic carbon formation", *Carbon*, v. 12, no 4, pp. 391–404.
14. Макаров, КИ, Печик, ВК, 1975, "Исследование кинетики термического превращения метана", *Кинетика и катализ*, т. XVI, вып. 6, сс. 1491–1500.
15. Теснер, ПА, Рафалькес, ИС 1952, "Исследование процесса образования углерода на поверхностях при термическом разложении углеводородов", *ДАН СССР*, т. 87, № 1, сс. 821–823.

16. Теснер, ПА 1977, "Двухстадийная модель образования пироуглерода и ее экспериментальная проверка", *ДАН СССР*, т. 235, № 2, сс. 410–413.
17. Теснер, ПА, Полякова, ММ, Михеева, СС 1969, "Кинетика образования углерода при термическом разложении метана на углеродной поверхности", *Труды ВНИИГАЗ, Переработка и использование природного газа.* вып. 40/48, сс. 8–21.
18. Теснер, ПА, Полякова, ММ, Михеева, СС 1978, "Кинетика образования пироуглерода при термическом разложении метана", ДАН *СССР*, т. 240, № 2, сс. 402–405.
19. Теснер, ПА, Робинович, БЯ, Матюшенко, ЛА 1977, "Изучение процесса сажеобразования при термическом разложении разбавленных смесей углеводородов", *Труды ВНИИГАЗ*, вып. 12/20, сс. 27–41.
20. Теснер, ПА, Городецкий, АЕ, Снегирева, ТД 1978, "Влияние водорода на структуру пироуглерода", *ДАН СССР*, т. 241, № 4, сс. 901–903.
21. Теснер, ПА, Городецкий, АЕ, Захаров, АП, Полякова, ММ 1979, "Образование пироуглерода из метана на кварце", *ДАН СССР*, т. 249, № 6, сс. 1379–1381.
22. Теснер, ПА, Головина, НБ, Городецкий, АЕ, Полякова, ММ 1976, "Кинетика образования пироуглерода из метана", *Химия твердого топлива*, № 1, сс. 129–135.
23. Коржов, ВП, Карпов, МИ, Прохоров, ДВ 2013, "Многослойные жаропрочные материалы на основе интерметаллических соединений ниобия и титана: получение, структура и механические свойства. (Multilayer heat-resistant materials based on intermetallic compounds of niobium and titanium: preparation, structure and mechanical properties)", *Scientific Proceedings of the Scientific-Technical Union of Mechanical Engineering, X International Congress «Machines, Technologies, Materials 2013*». Year XXI, vol. 10/147, September pp. 120–123.
24. Korzhov, Valeriy P, Karpov, Michael I, Prokhorov, Dmitriy V. 2013, "Structure evolution of multilayer materials of heat-resistant intermetallic compounds under the influence of temperature in the process of diffusion welding under pressure and their mechanical properties", *J. Intern. Scient. Public.: Materials, Methods and Technologies*, vol. 7, part 1, pp. 34–361.
25. Коржов, ВП, Карпов, МИ 2013, "Структура и высокотемпературная прочность при изгибе многослойного композитного материала из интерметаллидов титана с алюминием", *Вестник Тамбовского университета. Серия: естественные и технические науки*, т.18, вып. 4, сс. 1673–1675.
26. Коэффициент-диффузия-углерод. Большая Энциклопедия Нефти Газа. Режимдоступа: ngpedia.ru›id113773p1.html, свободный, – Заглавие с экрана. – Яз. рус.
27. Cook, J, Gordon, JE 1964, *Proceedings of the Royal Society*, v. 282, No 8, pp. 508.
28. Анищенков, ВМ, Милейко, СТ 1978, "Усталостное разрушение слоистого композита", ДАН *СССР*, т. 241, №5, сс. 1068–1069.
29. Kolchin, AA, Kiiko, VM, Sarkissyan, NS, Mileiko, ST 2001, "Oxide/oxide composites with fibres produced by using internal crystallization method", *Composite Science and Technology*, v. 61, No 7, pp. 1079–1082.